INTERNATIONAL JOURNAL OF CURRENT RESEARCH IN CHEMISTRY AND PHARMACEUTICAL SCIENCES
(p-ISSN: 2348-5213: e-ISSN: 2348-5221)
www.ijcrcps.com
(A Peer Reviewed, Referred, Indexed and Open Access Journal)
DOI: 10.22192/ijcrcps **Coden: IJCROO(USA)** **Volume 9, Issue 4 - 2022**

Research Article

DOI: http://dx.doi.org/10.22192/ijcrcps.2022.09.04.003

Development and study of electrode material for ammonia electrolysis to produce hydrogen

Dr. M. Surendra Varma[1], S.Prabu[2]

[1] Assistant professor, Department of Chemistry, PRIST Deemed to be University Thanjavur.
[2] M.Phil scholar, Department of Chemistry, PRIST Deemed to be University Thanjavur.

1. Abstract

Literature shows that, hydrogen production from ammonia electrolysis requires the development of improved catalysts for ammonia electro-oxidation [1-3]. In the past, several metals and alloys prepared by different method have been considered as potential catalysis [4]. It has been focused mostly on precious metal electrocatalyst for electro oxidation of ammonia. In the present work, studies have been carried on development of Nickel based non-noble electrode materials such as Nickel-sulfur, prepared by electrodeposition method for aqueous ammonia electrolysis [5-8]. Thiourea was used as sulphur source and some technological parameters on sulfur content of electrodeposited Nickel alloy was investigated in a modified watts bath. The surface structure, morphology and composition of Nickel alloy electrodes were observed using scanning electron microscopy (SEM) and Energy Dispersive X-ray Analysis (EDAX) method. The performance of these electrode materials in aqueous ammonia electrolysis at different operating conditions were evaluated by potentiodynamic polarization method.

Keywords: hydrogen production, ammonia electrolysis, electrodeposition, EDAX.

2. Experimental techniques

2.1 Preparation of Ni-S electrolytes:

The electrolyte used in the study is modified watt's bath containing thiourea as sulfur source. The electrolyte for nickel electrodeposition was prepared using double distilled water and its composition in the Table 3.1. The suspended impurities present in the solution were removed by filtration.

Table 2.1 Composition of Watt's bath

$NiSO_4.7H_2O$	40 gpl
$NiCl_2.6H_2O$	35 gpl
H_3BO_3	35 gpl
Thiourea	10-100 gpl
Temperature	40^0C

2.2 Surface pretreatment of mild steel substrate:

Before electroplating, the mild steel specimens were polished mechanically and degreased by acetone using cotton. These steps removed most of oils and impurities that may have been present on the surface of mild steel specimens. The specimens were cathodically and anodically cleaned in alkaline solution, using the following solution composition and operating conditions.

Sodium hydroxide	30 gpl
Sodium carbonate	30 gpl
Temperature	Room Temperature
Duration (cathodically)	2.0minutes
(anodically)	0.5 minutes
Current density	$50mA/cm^2$
Counter electrode	stainless steel

Organic particles present in the micropits or crevices will remain even after degreasing with organic solvent. When substrate is made as the cathode, the hydrogen evolved will help in removing the organic particles along with them. During this process, atomic hydrogen may get adsorbed on the surface and get on to the lattice that eventually leads to hydrogen embrittlement, which is removed when the substrate is made as anode.

The pretreated specimens were cleaned with distilled water before electro deposition process.

2.3 Electrodeposition of Ni-S on mild steel substrate:

Electrodeposition of Ni-S alloy was carried out on pretreated mild steel specimen of 9X4X0.2 cm dimension with pure (99.99%) nickel mesh anode of equal size using the above electrolytes [9-10]. The exposed area for electrodeposition was 8X4X0.2 cm and other areas were masked with maskent. The specimens were weighed before and after electrodeposition using digital electronic balance. Pretreated mild steel specimens were placed into beaker containing 250 ml of bath (with and without thiourea) were electroplated at different current densities and thiourea concentration at 40^0C. The duration of plating process was 30 minutes. The cathode current efficiency for nickel electrrodeposition was calculated using the following relation.

$$\text{Cathode current efficiency} = \frac{w \times 100}{W}$$

Where 'w' is the weight of the deposit, 'W' theoretically expected weight.

Theoretical expected weight can be calculated using the following formula.

$$\text{Theoretical weight} = \frac{\text{Current passed (A)} \times \text{Duration (hrs)} \times \text{Eq. Wt. of } Ni^{2+}}{26.8 \text{ A.hr}}$$

3.4 Characterization

The two different methods were employed to characterize the prepared electrode materials

3.4.1 Physical characterization

The surface morphology and composition of the prepared electrodeposits were analysed using Scanning Electron microscope (SEM) and Energy Dispersive X-ray Analysis (EDAX) method[11-12].

3.4.1.1 Scanning Electron Microscopy

SEM is a class of electron microscope that images the sample surface by scanning it with a high –energy beam of electrons in a raster scan pattern. The electrons interact with the atoms that make up the sample producing signals that contain information about the samples surface topography, composition and other properties such as electrical conductivity[13-15].

The types of signals produced by an SEM include secondary electrons; back scattered electrons (BSE), characteristic X-rays, light (acthodoluminescence), specimen current and transmitted electrons. These types of signals all require specialized detectors that are all not usually present on single equipment. The signals result from interactions of the electron beam with atoms at or near the surface of the sample [16-20]. In the most common or standard detection mode, secondary electron imaging or SEM, the SEM can produce very high-resolution images of a sample surfaces, revealing details about 1to 5mm in size. Due to the way these images are created, SEM micrographs have a very large depth of field yielding a characteristic three-dimensional appearance useful for understanding the surface morphology of a sample.

A wide range of magnifications is possible, from about X 25 (about equivalent to that of a powerful hand –lens) to about X 250000 about 250 times the magnification limit of the best light microscopes.

Scanning Process

In a typical SEM, an electron beam is thermionically emitted from an electron gun fitted with a tungsten filament cathode. Tungsten is normally used in thermionic electron guns because it has the highest melting point and lowest vapour pressure of all metals, thereby allowing it to be hated for electron emission, and because of its low cost.

The electron beam, which typically has energy from a few hundred ev to 40 Kev, is focused by one or two condenser lenses to a spot about 0.4 nm to 5 nm in diameter. The beam passes through pairs of scanning coils or pair of deflector plates in the electron column, typically in the final lens, whilch deflect the beam in x and y aces so that it scans in a rastser fashion over a rectangular area of the sample surface.

3.4.1.2 Energy dispersive X- ray spectroscopy:

Energy dispersive x-ray spectroscopy (EDS, EDX or EDXRF) is an analytical technique used for the elemental analysis or chemical characterization of a sample. It is one of the variants of XRF. As a type of spectroscopy, it relies on the investigation of a sample through interactions between electromagnetic radiation and matter, analyzing x-rays emitted by the matter in response to being hit with charged particles [21-24]. Its characterization fundamental principle that each element has a unique atomic structure allowing x-rays that are characteristic of an elements atomic structure to be indentified uniquely from each other.

To stimulate the emission of characteristic X- rays from a specimen, a high energy beam of charged beam of particles such as electrons or protons, or a beam of X-rays, is focused into the sample contains ground state (or unexcited) electrons ion discrete energy levels or electron shells bound the nucleus.

The incident beam may excite an electron in an inner shell, ejecting it from the shell while creating an electron hole where the electron was an electron from an outer, higher- energy shell than fills the hole, and the difference in energy between the higher- energy shell and the lower energy shell may be released in the form of an X-ray.

The number and energy of the X-ray emitted from a specimen can be measured by an energy dispersive spectrometer. As the energy of the X-rays is characteristic of the difference in energy between the two shells, and of the atomic structure of the element from which they were emitted, this allows the elemental composition of the specimen to be measured.

3.4.2 Electrochemical characterization

Potentiodynamic polarization studies

The potentiodynamic polarization experiments were performed by a CH100A – Electrochemical analyzer using three electrode cell assemblies. A Ni-S alloy of 1 cm^2 area was used as the working electrodes. $Hg/HgO/OH^-$ electrode was used as the reference electrode, and a large Pt foil was employed as the counter electrode [24-27]. A Lug gin capillary, whose tip was set at a distance of about 1 mm from the surface of the working electrode, was used to minimize the variations due to IR drop in the electrolytes [28-31]. The aqueous ammonia of various concentrations with potassium hydroxide was used as electrolyte. The potential was scanned from 0 to 1.0 V with the scan rate of 0.01 V/sec.

Results and Discussion

3.1 Electrodeposition of Nickel sulfur alloy

3.1.1 Effect of operation cathode current density on Plain Nickel electro deposition efficiency

The dependence of plain Nickel deposition efficiency using sulphate bath (without thiourea) as a function of cathode current densities is shown in figure 4.1. The cathodic nickel deposition efficiencies decrease from 98.52% to 92.03% with increasing operating cathode current density. It may be attributed to parasitic reaction such as hydrogen gas evolution from the acidic sulphate electrolyte, as current rises, the cell potential decreases, encouraging hydrogen evolution.

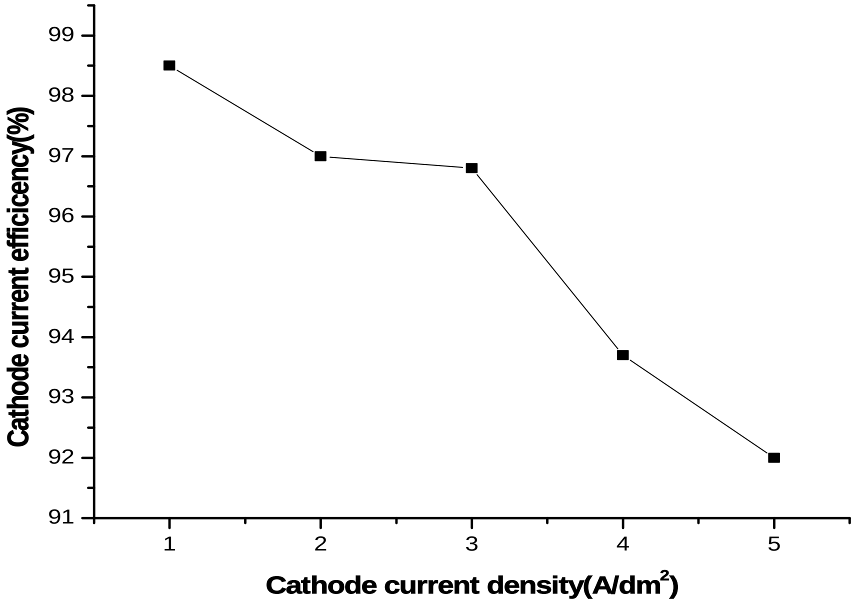

Fig 3.1 Effect of operating cathode current density on Plain Nickel electrodeposition efficiency

3.1.2 Influence of various factors on sulfur content

3.1.2.1 Effect of Thiourea Concentration

Electrodeposition of Nickel-Sulfur alloy was carried out at the cathode current density of 2A/ dm^2 in room temperature with various thiourea concentrations in the electrolyte. Fig 4.2 shows the effect of thiourea concentration (10-200 g/l) on the sulfure content in the Ni-S deposit. From the figure it is understood that the increase in thiourea concentration increase the sulfur content significantly. When thiourea concentration is lower than 150 g/l, the sulfur content increases steeply. However, thiourea concentration above 150 g/l has only little effect because very high thiourea concentration is invalid and some precipitation appears in solution since its solubility is limited in nickel electrolyte.

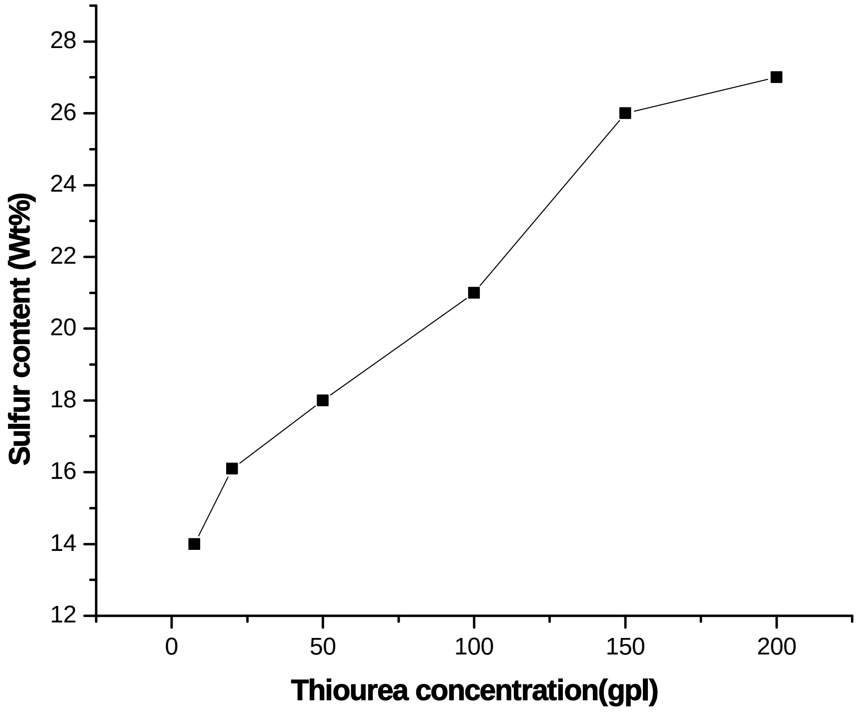

Fig 3.2 Influence of thiourea concentration on the sulfur content in the Ni-S electrodeposits at $2A/dm^2$

3.1.2.2 Effect of Current Density

Fig 4.3 shows the effect of operating cathode current density (1-4 A/dm^2) on the sulfur content in the electrolyte containing 100gpl thiourea concentration. The result shows that the sulfur content decreases as the current density increases from 1 to 4 A/dm^2. This can be explained by polarization behavior in electrodepositing solutions. Partial Ni^{2+} ions are complexed with thiourea in the form of Ni $[CS(NH_2)_2]^{2+}$. As current density increases, the polarization of Ni $[CS(NH_2)_2]^{2+}$ ions increases and the rate of its precipitation decreases. Thus much more nickel is deposited and so the sulfur concentration reduces.

These results indicate that the operating parameters and electrolyte compositions playing significant role in Nickel-Sulfur alloy electrodepositing process. Then the obtained Nickel- sulfur electrodeposits were subjected into surface and electrochemical characterization for its performance evaluation in aqueous ammonia electrolysis.

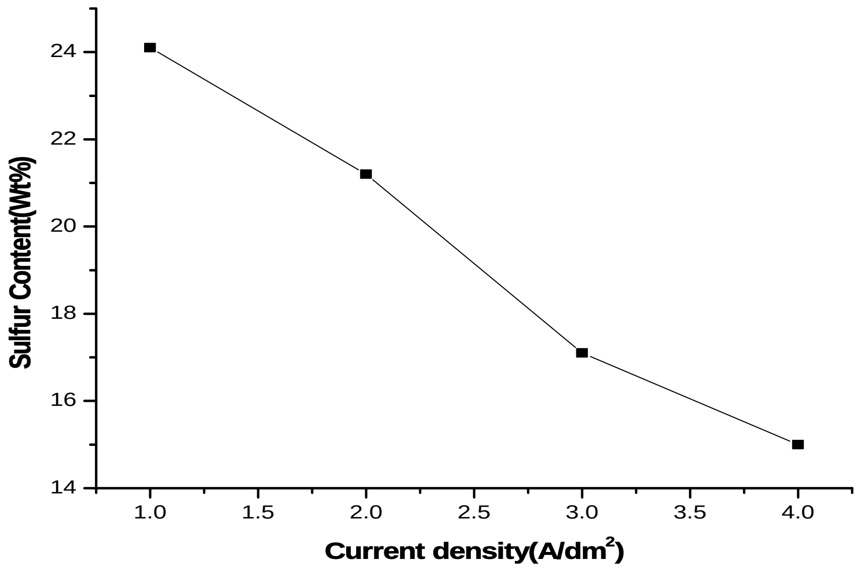

Fig 3.3 Influence of cathode current density on the sulfur content in the Ni-S deposits at 100 gpl thiourea concentration

3.3 Scanning Electron Microscopy

SEM micrographs of the surface topography of the Nickel-Sulfur alloy with two different (10 gpl and 200 gpl TU concentration) sulfur contents are shown in fig 4.4. It shows that surfaces become smoother while sulfur content increases from 14.18% to 27.12%. When the sulfur content is lower, lots of global particles lie on the surface of Ni-S electrodeposits which represent nickel crystals. As sulfur content grows, the particles disappear considerably and the surface becomes smooth at 27.12 mass% which corresponds to amorphous composition and would enhance the electrochemical activity in aqueous ammonia electrolysis process.

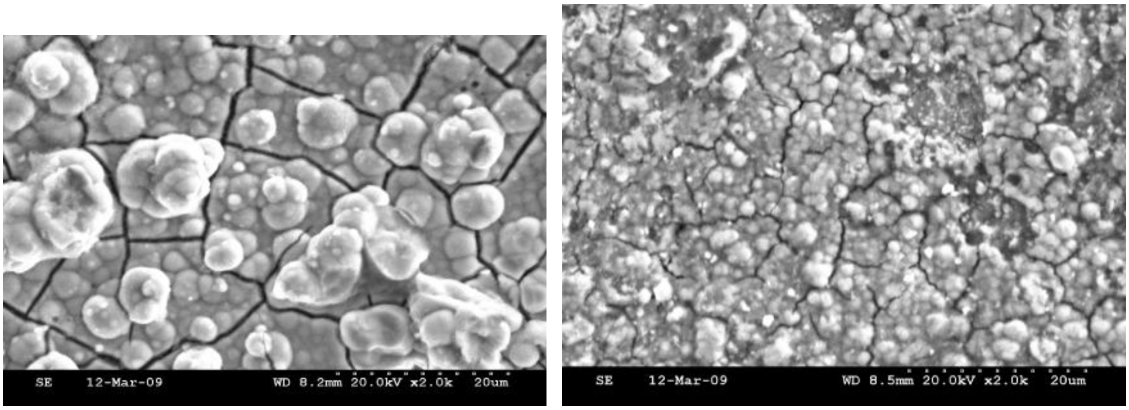

(a) **(b)**

Fig 3.4 SEM image of Ni-S alloy with (a) 10 gpl (b) 200 gpl thiourea concentration

3.3. Performance evaluation of Nickel alloy electrodes in aqueous ammonia electrolysis

The electrodeposited Nickel alloy electrodes were subjected into aqueous ammonia electrolysis and its performance was evaluated by performing potentiodyamic polarization studies at different operating conditions.

3.3.1 Influence of sulfur content in the electrodeposits for ammonia oxidation

Fig 4.5 shows the polarization curves of nickel electrode prepared of various % of sulfur content in the electrodes at room temperature. It is apparent that the influence of sulfur content on oxidation of ammonia is significant in alkaline medium. With increasing sulfur content, the current density for ammonia oxidation increases at a particular potential (beyond it's on-set potential for oxidation). It is also observed that the onset potential for ammonia oxidation is reduced to about 100-200 mV, while sulfur content increases in the electrode (14.18 % to 27.12%), for higher sulfur content. The lowest electrocatalytic activity is observed for Nickel electrode with 14.18% sulfur. When compared with other electrodes showing it's higher over potential for ammonia oxidation. The maximum current density obtained on Ni-S (27.12%) at 33^0C was about two times larger than observed on Ni-S (14.17%) electrode.

It can be explained in view of the mechanism proposed by Gevischer and Manerer

$$NH_{3ads} + OH^- \rightleftharpoons NH_{2ads} + H_2O + e^- \qquad (1)$$

$$NH_{2ads} + OH^- \rightleftharpoons NH_{ads} + H_2O + e^- \qquad (2)$$

$$NH_{ads} + OH^- \rightleftharpoons N_{ads} + H_2O + e^- \qquad (3)$$

$$NH_{x\,ads} + NH_{y\,ads} + (x+y)OH^- \rightleftharpoons N_2 + (x+y)H_2O + (x+y)e^- \qquad (4)$$

$$2N_{ads} \rightleftharpoons N_2 \qquad (5)$$

At low current densities the oxidation of surface amine is consider to be rate limiting equation 2 , where as at higher current densities the recombination of adsorbed nitrogen is the limiting step. N_{ads} accumulate at the surface of the electrode blocking the active site of the catalyst and therefore acting as poison towards the reaction. The absorbed increased electro catalytic active in the present study may be attributed to its ability to change the energetic of the surface site to inhibit or promote the sorption species resulting lower over potential. The maximum electro catalytic activity was observed for electrode with sulfur content of 27.12%.due to this amorphous nature as evident by the SEM picture. Further experiments were carried and with this electrode, to study the influence of other operating parameter like temperature.

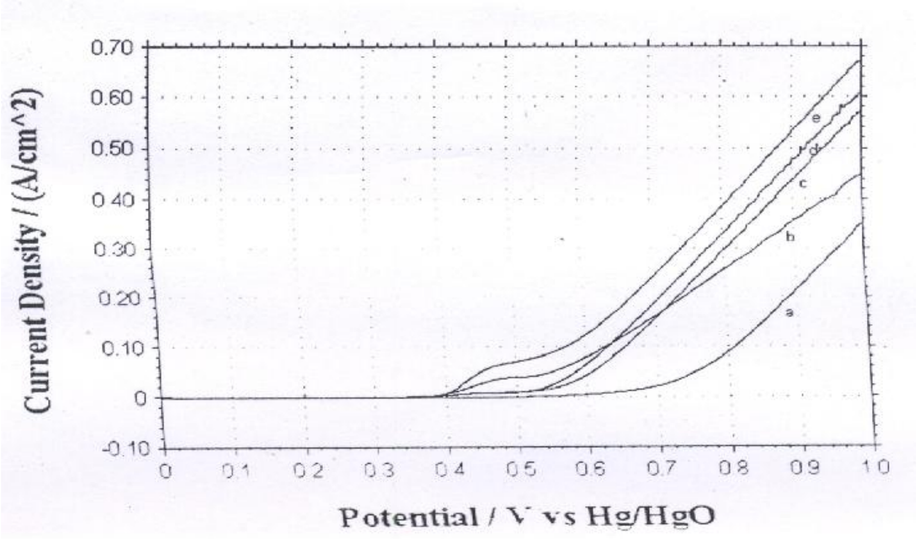

Fig 3.5 **Potentiodyamic polarization curves of various Ni-S alloy electrodes for ammonia electrolysis in 1M NH_3+5 M KOH solution at room temperature. Sulfur content (%) (a) S- 14.04 (b) S- 18.14 (c) S- 21.14 (d) S- 26.01 (e) S- 27.12**

3.3.2 Influence of operating temperature

The influence of operating temperature on aqueous ammonia electrolysis was studied using Ni-S (26.01 %) electrode at four different temperature and the polarization results are shown in Fig 4.6. It is apparent that the influence of temperature on electro chemical activity of Nickel- sulfur electrodes is significant in alkaline solution. With increasing in temperature the hydrogen overvoltage decreases. This is because increasing temperature can enhance the catalytic activity of electrode. Lower value of electrode potential will be more advantageous from the point of view of minimizing activation over potential and lower energy consumption for ammonia oxidation.

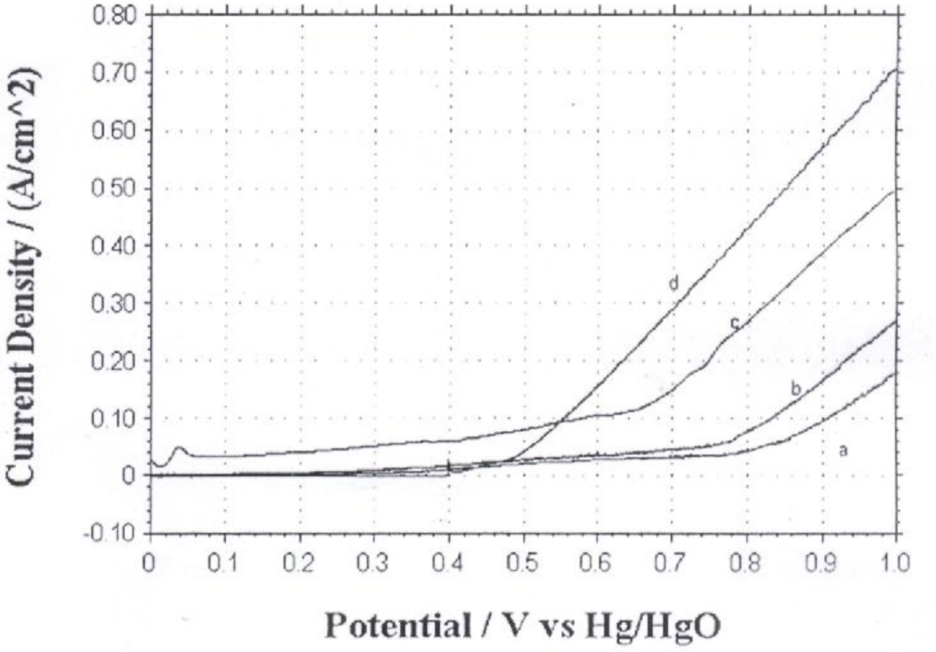

Fig 3.6 Potentiodyamic Polarization curves of amorphous Ni-S electrode at various temperatures (a)Room temp (b) 50°C (c) 70°C (d) 80°C

From the above studies, we may deduce that the activity of electrodeposited nickel-alloy electrodes (such as Ni-S), depends on the degree of the amorphous state of the electrode for aqueous ammonia oxidation. It is more or less obvious that the role of the non metallic element in amorphous alloys of nickel consist mainly in that it alloys the formation of amorphous structure of the layer. Although, it was not the purpose here to develop optimized catalyst, it is seen that Ni-S alloy electrodeposits behaves better for aqueous ammonia oxidation process resulting lower overvoltage at particular current density region The presented results explore that, the likelihood of electrolyzing the aqueous ammonia for hydrogen production using non precious metal alloy catalysis such as Ni-S, which widely used in alkaline water electrolysis.

4. Conclusion

Materialization of a hydrogen economy could provide a solution to significant global challenges. In particular, the possibility of improving the efficiency and simultaneously minimizing the environmental impact of energy conversion process, together with the opportunity to reduce the dependency of fossil fuels, are main drivers for the currently increasing research and development efforts.

The present study shows the electrolysis of ammonia is a potential technology for the on-board production of hydrogen. Here are some concluding remarks as drawn from this study.

1 The development of electrode by electro deposition appears to be a efficient technique for ammonia electrolysis.
2 For electro deposition Ni-S alloy, the thiourea concentration and the operating current density are the key factors influencing the sulfur content in the electro deposits.
3 SEM examinations shows (Ni-S) that the structure of Ni-alloy electrodeposits is amorphous.
4 The electro chemical activity of amorphous Ni -alloy electrode increases with temperature during course of ammonia electrolysis.

The results of the study indicate that the production of hydrogen by the electrolysis of NH_3 is promising technology as the thermodynamics is in favor of the reaction. However the commercialization of the technology depends on the development of effective electrodes for the electro-oxidation of NH_3. Therefore, future work on this area should be focus on the further development of electrode to reduce the over potential of this reaction.

References

1. E.Raub and K.Muller,’Fundamentals of metal deposition‘ Elsevier publication, Amsterdam-London –New York, **1967**.
2. L.Hampel, ‘The Encyclopedia of Electrochemistry’, Reinhold publishing corpn., NY, **1964**, 14.
3. M.Paunovic and M.Schlesinger. ‘Fundamentals of Electrochemical Deposition’ Willey publication New York, **1998**.
4. F.C.Walsh, Trans.Inst. Metal Finish, **1991**, 69(4), 155.
5. Des Barker and F.C.Walsh, Trans.Inst. Metal Finish, **1991**, 69(4), 158.
6. comprehensive Treatise of Electrochemistry **1981**, 2.
7. Dragica Li.Stojic, Milica P. Marca eta, Sofija P. Sovilj, S c epan S.Miljanic. J.Power Sources **2003,** 118, 315.
8. C.J.Winter, J.Nitsch (Eds.), Springer, Berlin, **1988**.
9. D.Lj. Stojic, S. Miljanic, T.D. Grozdic, N.M. Bibic, M.M. Jaksic, Int. J.Hydrogen Energy, **1991**, 16(7), 469.
10. R. Friedland, W. Smith, A. Speranza,. Integrated Renewable Hydrogen Utility System, Phase I Final Technical Report and Market Assessment PES-T-99014, **2000**.
11. Y.Misumi, H. Michishita, H. Matsumoto, T. Ishihara, Materials Science & Engineering, **1989**, 99, 434.

12. E.Laouini, M. Hamdani, M.I. S. Pereira, J. Douch, M.H. Mendonca, Y. Berghoute, R.N. Singh, J. Appl.Electrochem, **2008**, 38, 1485.
13. J. Yang, J. Li, H. Lin, X. Yang, X. Tong , G.Guo, J. Appl.Electrochem, **2006**, 36, 945.
14. H. Dumont, P.W. Wrona, J.M Lalancette, H. Minard, J. Appl.Electrochem, **1992**, 22, 1049.
15. J.Y. Huot, L.Brossard, J. Appl.Electrochem, **1990**, 20, 281.
16. D.W. Kirk, S.J. Thorpe, H. Suzuki, Int. J. Hydrogen Energy, **1997**, 22(5), 493.
17. J.M. Jaksic, N.M. DRistic, N.V. Krstajic, Int. J. Hydrogen Energy, **1998**, 23(12), 1121.
18. Q. Han, K. Liu, J. Chen, X. Wei, Int. J. Hydrogen Energy, **2003**, 28, 1207.
19. Frederic Vitse, Matt Cooper, Geradine G.Botte, J.Powersources, **2005**, 142, 18.
20. Matthew Cooper and Gerardine G.Botte. J.Electrochemical society, **2006**, 153 (10) A1894.
21. K.Yao,Y.F.Cheng J.Powersources, **2007**,173.
22. K.Yao,Y.F.Cheng J.Materials Chemistry, **2008**, 108, 247.
23. Kazuki Endo, Kydo Nakamura, Yasushi Katayama, Takashi Miura, J. Electro chemical Act, **2004**, 149, 2503.
24. B.A.Lopez deMishima, D.Lescano,T.MolinaHelgado and H.T. Mishma, J. Electro chemical Act, **1998**, 43, 395.
25. M. Donten, W. Hyk, M. Ciszkowska, Z. Stejek, J.Electroanalysis, **1997**, 9.
26. M. Soledad, V. Zanartu, C. Yanez , J.Electroanalytical Chemistry, **1996**, 405,159.
27. I. Paseka, J. Electro Chemical Act., **1995**, 40, 1663.
28. J.C. Ganley, E.G. Seebaver, R.I. Masel, J.Powersources, **2004**, 37, 53.
29. A..C.A.devooys,M.F.Mrozek,M.T.m.Koper,R.A.Van Santen,J.A.R.Vanveen M.J.Weaver, Electrochemistry Communications, **2001**, 3, 293.
30. W.K. Hu, Y.S. Zhang, D.Y. Songd, Funct Mater, **1995**, 26 , 456.
31. I.A.Raj, J.Appl.Electrochem., **1993**, 28, 4375.

Access this Article in Online	
	Website: www.ijcrcps.com
Quick Response Code	Subject: Chemistry
DOI: 10.22192/ijcrcps.2022.09.04.003	

How to cite this article:

M. Surendra Varma, S.Prabu. (2022). Development and study of electrode material for ammonia electrolysis to produce hydrogen. Int. J. Curr. Res. Chem. Pharm. Sci. 9(4): 21-30.

DOI: http://dx.doi.org/10.22192/ijcrcps.2022.09.04.003